FACIAL NORMAL MAP CAPTURE USING FOUR LIGHTS

An Effective and Inexpensive Method of Capturing the Fine Scale Detail of Human Faces using Four Point Lights

Jasenko Zivanov, Pascal Paysan, Thomas Vetter
Computer Science Department, University of Basel, Bernoullistrasse 16, 4056 Basel, Switzerland
jasenko.zivanov@stud.unibas.ch, pascal.paysan@unibas.ch, thomas,vettr@unibas.ch

Keywords: face rendering, face normal map, normal map capture, surface reconstruction

Abstract: Obtaining photorealistic scans of human faces is both challenging and expensive. Capturing the high-frequency components of skin surface structure requires the face to be scanned at very high resolutions, outside the range of most structured light 3D scanners.
We present a novel and simple enhancement to the acquisition process, requiring only four photographic flash-lights and three texture cameras attached to the structured light scanner setup.
The three texture cameras capture one texture map (luminance map) of the face as illuminated by each of the four flash-lights. Based on those four luminance textures, three normal maps of the head are approximated, one for each color channel. Those normal maps are then used to reconstruct a 3D model of the head at a much higher mesh resolution, in order to validate the normals. Finally, the validated normals are used as a normal map at rendering time. Alternatively, the reconstructed high resolution model can also be used for rendering.

1 INTRODUCTION

Humans are exceedingly adept at detecting errors in computer-generated faces, as we have a lifetime of experience observing real ones. At the same time, faces are among the objects one would most often want to render, as they provide a unique way to reach out to an audience and communicate ideas and impressions.

Two things make the realistic rendering of faces difficult. One is fine scale skin detail, visible almost exclusively by the influence it has on shading patterns, the other is its translucency, and especially the fact that skin is far more translucent under red light than under green or blue light [Jensen et al., 2001].

While there are means of capturing high resolution detail in entire faces, they are limited to exceptionally precise range scanners and light domes containing thousands of light sources, both of which are rather expensive. Our approach sacrifices some precision in order to perform the same task by using only four point light sources. Care is taken, however, not to impair the visual quality of the result - images rendered using the resulting model or normal maps remain visually credible, even if they do not allow for an exact reconstruction of a photograph of the same head.

By estimating a separate normal map for each color channel, we can also capture some effects of subsurface scattering. Since red light tends to travel further inside skin before leaving it than green or blue light, skin appears smoother when observed under red light. As a consequence, darker points on the skin surface appear more red than lighter points.

2 RELATED WORK

Barsky and Petrou [Barsky and Petrou, 2001] present a normal estimation technique somewhat similar to ours. They offer a method to estimate the normals of a non-translucent lambertian surface by evaluating photographs taken under different simple illumination conditions. De-

viations of the surface from a lambertian reflectiveness, caused by both an inhomogenous distribution of incoming light and the non-lambertian reflectance of the material itself, introduce an error in the lower frequency bands of the resulting normal map. An example of this can be seen in Fig. 1.(b).

Nehab et al [Nehab et al., 2005] present a method to combine the low frequency bands of a range scanned model with higher frequencies obtained through photometric stereo. The method is aimed at the capture of smaller objects, though, and does not appear suitable for human faces. Weyrich et al [Weyrich et al., 2006] apply the two methods to capture high resolution meshes of faces. In contrast to us, however, they use well above 1000 light sources, each of which has been painstakingly calibrated by taking photographs of a disk of Fluorilon, a material with an almost ideally lambertian reflectiveness, at different positions inside the individual light cones.

Haro et al [Haro et al., 2001] use silicone molds of skin to acquire normal maps of patches of the facial surface, and then grow the resulting pattern to cover the entire face using a texture synthesis technique. The approach is unable to capture local fine scale features specific to a person such as wrinkles, moles and scars. It also ignores the translucency of skin, although its effects could be computed at render time, for example through the use of texture space convolution as in [Borshukov and Lewis, 2003]. Using the geometrically correct normal maps without addressing the effects of translucency, however, leads to grainy-looking and sandpaper like skin.

Debevec et al [Ma et al., 2007] offer a scanning technique that produces four independent normal maps, one for the diffuse reflection in each of the three color channels and one for specular reflections. The lighting setup they use is fairly complex though, as the technique relies on polarized full sphere illumination.

3 SETUP

We use a structured light 3D scanner system for the geometry acquisition. The texture is captured using three high resolution SLR cameras and four photographic flash lights. The flash lights have an effect on the face similar to that of theoretical point lights.

The positions of the flash lights have been determined by scanning a number of taut strings running together at each of the lights and intersecting the measured lines in space. When choosing where to place the lights, care has been taken to maximize areas of the face lit by at least three lights.

The light intensity distributions of the light cones do not need to be known, as long as the light intensity varies only smoothly along the surface. If this is the case, the light intensity can only have an impact on the low frequency component of the estimated normals, while only the high frequencies are taken from the photographs - the low frequencies can be extracted from shape.

4 PROCEDURE

After scanning the face using the structured light capture process, which takes about half a second, the four flash lights are triggered in quick succession, and four images are captured by each of the three cameras. The overall scanning process takes approximately three seconds.

The twelve photographs are then mapped into the head's texture space, resulting in twelve texture maps. Ray tracing is applied to calculate the self-occlusion of the face in regard to the cameras and the light sources.

Before the normal estimation process is initiated, the four sets of three images are used to reduce the effects of specularity. This is done by forming minima over the triples of textures captured by the three cameras under each of the four lights.

We are then left with only four textures of the face, one for each light source. As most areas of the face contain shadows in at least one of the textures, we estimate most of the normals based on three color values.

Those normals carry a systematic bias due to the varying intensity of incoming light across the face, as our light sources are in reality photographic flash-lights that spread light inside a cone, and not perfect point lights. That bias is removed by ensuring that the average normal direction in a certain area is perpendicular to the surface of the 3D model in that area.

Finally, photographic noise is removed from the normal maps by reconstructing the 3D-surface at the resolution of the normal maps, and using the normals implied by that surface. The surface itself can also be used as a high-resolution model of the face.

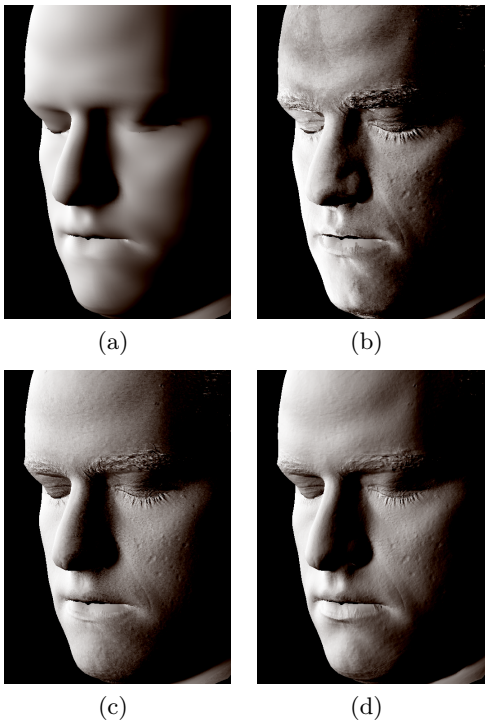

Figure 1: Outline of the capture process. The initial normals (a) are calculated from the geometry of the mesh. The positions of multiple vertices are taken into account when the normal of each vertex is computed, thus the smooth appearance. Photographs of the face are used to estimate the raw normal maps (b). Low frequencies from (a) and high frequencies from (b) are combined to compute the corrected normal map (c), which is then used to reconstruct a high resolution surface, yielding the final reconstructed normal map (d).

5 SPECULARITY REDUCTION

Specularity is considered a necessary evil in our approach. Although it carries the most precise normal information (as specularly reflected light does not succumb to subsurface scattering), the coverage of the face by intense specularity in our setup is simply insufficient to allow for a stable estimation of specular normals and the spatially varying specular reflectance function.

Let P_{icl} be pixel i of the radiance texture of the head taken by camera c under light l. Essentially, what we are interested in, is the value $P_{il} := min_c(P_{icl})$. As diffusely reflected light is assumed to spread out evenly in all directions, while specularly reflected light is focused in one particular direction, looking at a point on the surface from the direction from which it is seen the darkest, also yields the color closest to the diffuse color of the surface at that point.

Forming the minimum in this naive way would however create discontinuities in image color at visibility borders and introduce edges into the resulting normal map. In order to avoid this, the borders are interpolated smoothly, using an offset negative gaussian of the distance of each texel to the border as its weight.

The suppression of specularity could also be performed using cross polarization, ie. placing polarizing filters in front of the camera and the light source, though great attention would have to be paid to the orientation of the filters, as the cameras and the light sources are not located in a plane in space.

Now that specular reflections have been removed from the input textures, those textures can be used to estimate normal maps.

5.1 Normal Estimation

After our specularity reduction step, we are left with four images of the the diffuse radiance of the head, as seen under the four light sources.

Assuming lambertian reflection, we can express the luminance of color channel $\lambda \in \{R, G, B\}$ of texel i under light l as a dot product of $\vec{N_{i\lambda}}$, the normal we are looking for, and $\vec{L_{il}}$, the normalized vector pointing towards the light, scaled by the surface albedo $a_{i\lambda}$:

$$I_{il\lambda} = a_{i\lambda} \cdot \vec{L_{il}} \cdot \vec{N_{i\lambda}}$$

If the texel is in shadow under only one light, which is mostly the case, we can simply solve the following linear system of equations, once for each color channel:

$$a_{i\lambda} \cdot \begin{pmatrix} \vec{L_{i0}}^{\mathrm{T}} \\ \vec{L_{i1}}^{\mathrm{T}} \\ \vec{L_{i2}}^{\mathrm{T}} \end{pmatrix} \cdot \vec{N_{i\lambda}} = \begin{pmatrix} I_{i0\lambda} \\ I_{i1\lambda} \\ I_{i2\lambda} \end{pmatrix}$$

Note that we are only interested in the direction of $\vec{N_{i\lambda}}$ at this point, so the value of $a_{i\lambda}$ that only scales the normal can be ignored.

What remains is a linear system of equations with three unknowns and three equations. If the texel is visible under all four lights, we even have an overdetermined linear system of the same form, that we can solve in the least squares sense. Due to our setup, the overdetermined texels usually form a thin vertical band in the middle of the face.

Either way, solving the system yields the scaled normal $a_{i\lambda} \cdot \vec{N}_{i\lambda}$. We could hypothetically keep the length of $a_{i\lambda} \cdot \vec{N}_{i\lambda}$ as the value of $a_{i\lambda}$, but doing so would introduce irregularities in facial color, as the normal $\vec{N}_{i\lambda}$ still suffers from a low frequency error. Instead, we only normalize the resulting normal.

5.2 Low Pass Correction

The resulting normal maps still suffer from a systematic low frequency error caused by the inhomogenous distribution of incoming light and deviations from lambertian reflection (see Fig 1.(b) for an example). That error can be reduced by discarding the low frequency part of the normal map and replacing it with the low frequency data from the 3D model. We call that process the low pass correction.

The low pass correction is performed separately for the five facial areas - the four areas illuminated by all but one of the four lights, and the area illuminated by all four lights. The reason for this is that the five areas exhibit different low frequency errors, as the error caused by each light nudges the estimated normal in a different direction.

Let N_{sharp} be the normal map we have just obtained, N_{blur} a low-pass filtered version of that normal map and N_{vertex} a low-pass filtered normal map generated from the 3D geometry, which is created by rendering the vertex normals into texture space.

We define a new normal map N_{comb} as follows:

$$N_{comb} := N_{sharp} + N_{vertex} - N_{blur}$$

N_{comb} has the useful property that when it is itself low-pass filtered, the result is very close to N_{vertex} - the low frequencies of N_{comb} consist of information from N_{vertex}, while only the high frequency information is taken from N_{sharp}. This is highly useful, as variations in incoming light intensity are always of a low frequency nature.

Since the correction is performed on each vector component independently, the resulting normals have to be renormalized.

Our method is similar to the one presented in [Nehab et al., 2005], except that we perform the low-pass filtering by convolving the normal map linearly with a gaussian kernel, instead of estimating a rotation matrix for each normal - we assume that the difference in the lower frequency bands is small enough for that not to make any difference.

Once the five patches of N_{comb} have been computed for all five areas, they can be safely put together - because they all share the same low frequency information, there is no longer any danger of edges (discontinuities in the normal map) appearing at the seams.

At points illuminated by only two or less lights (the sixth area), the original vertex normal map, N_{vertex}, is used.

After the low pass correction, the normal map looks like Fig. 1 (c). In order to render images with it, a texture containing the surface albedo is needed. The albedo a_λ for color channel λ is defined as the ratio of light of color λ that is reflected off a surface, when the incoming light direction is perpendicular to it.

5.3 Albedo Estimation

Only after the low pass correction has been completed, is it safe estimate the surface albedo.

We define the albedo $a_{i\lambda}$ for texel i and color channel λ as follows:

$$a_{i\lambda} = \frac{\sum_{valid\, l} (\vec{L}_{il} \cdot \vec{N}_{i\lambda}) I_{il\lambda}}{\sum_{valid\, l} (\vec{L}_{il} \cdot \vec{N}_{i\lambda})^2}$$

$\vec{N}_{i\lambda}$ is the estimated surface normal at texel i for color channel λ, $\vec{L}_{il}$ is the normalized vector towards light l and $I_{il\lambda}$ is the λ channel of the diffuse luminance of texel i under light l. The expression can be seen as a weighted average over the individual contributions $I_{il\lambda}/(\vec{L}_{il} \cdot \vec{N}_{i\lambda})$, weighted by the squared lambert factors $(\vec{L}_{il} \cdot \vec{N}_{i\lambda})^2$. The weights are squared in order to suppress the influence of dark pixels, where the relative error is the largest.

At the end, the albedo is grown into areas where it is undefined. This is done so tiny cracks can be removed that can form mostly around the lips, where occlusion is critical and the texture resolution is low (in our case). This is done by setting the value of each undefined pixel to the average value of all defined neighboring pixels (after which the pixel becomes defined), and repeating the procedure a number of times.

Although the data computed so far is sufficient to render images, the quality of the normal maps can still be improved. This is done by computing a 3D surface at the resolution of the normal map with surface normals that match those of the

normal map as closely as possible. The normals of that surface are then used as a more realistic normal map.

5.4 Surface Reconstruction

Not every vector field is a possible normal map - at least not as long as the surface it is supposed to represent has been adequately filtered prior to sampling.

We are looking for a normal map that actually corresponds to a real surface. By enforcing that fact, we can remove part of the photographic noise that has found its way into the normals without sacrificing higher frequency bands of the normal map. We do that by reconstructing the surface at the resolution of the normal map. The reconstructed surface can then be either rendered directly or its surface normals can be written into a normal map, and the original, coarse mesh rendered using that normal map.

If the normal map is to be used with the coarse mesh, the normal maps for all three color channels have to be used to reconstruct three different meshes. If the high resolution mesh is to be used for rendering, only one of the meshes has to be reconstructed, preferrably the one corresponding to the green channel. The effects of subsurface scattering on the color of skin are thereby lost. The green channel is chosen because it offers the best trade-off between signal intensity and contrast, because the normals corresponding to the red channel are much softer, while the ones corresponding to the blue channel are noisy as only very little blue light is reflected off human skin.

The surface reconstruction is again similar to [Nehab et al., 2005], although we use an iterative non-linear method instead of attempting to deal with a $10^6 \times 10^6$ (albeit sparse) matrix. The size of the problem stems from the fact that the displacement of each texel is given by the normal map only as relative to its neighboring texels.

Our procedure looks as follows:

Let N_{comb} be the original normal map, and P_0 a texture holding the 3D positions of each texel. P_0 is defined in such a way that an entry $P_0(x, y)$ holds the 3D position of the surface between the four normal map entries $N_{comb}(x, y)$, $N_{comb}(x + 1, y)$, $N_{comb}(x, y + 1)$ and $N_{comb}(x + 1, y + 1)$, as illustrated in Fig. 2.

Furthermore, for each texel $P_0(x, y)$, a corresponding axis $A(x, y)$ is defined, parallel to the interpolated vertex normal at that point. It is along that axis, that the position $P_0(x, y)$ is allowed to move.

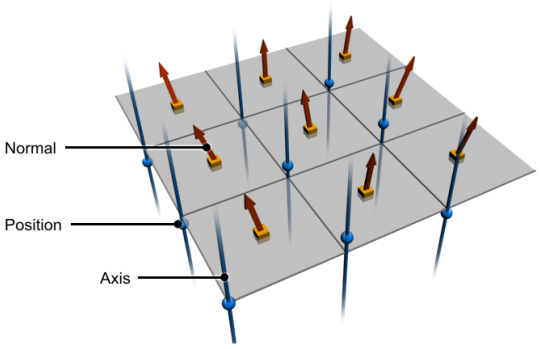

Figure 2: The setup for our surface refinement process. Note that the positions are placed between the normals of the normal map.

The position $P_{i+1}(x, y)$ for each successive iteration is obtained using the following algorithm:

Algorithm 1: Geometry Refinement

for $i \in \{0 \dots iterations\}$ **do**
  for $(x_t, y_t) \in texels$ **do**
1 `error[`x_t, y_t`] = 0;`
    for $(x_s, y_s) \in neighborhood(x_t, y_t)$ **do**
2 `n =` `normal_between(`$(x_s, y_s), (x_t, y_t)$`);`
3 ϵ `=` $\frac{\text{dot}(P_i[x_t,y_t]-P_i[x_s,y_s],n)}{\text{dot}(A[x_t,y_t],n)}$`;`
4 `error[`x_t, y_t`] +=` weight$(x_s, y_s) \cdot \epsilon$`;`
5 `avg_error = gauss_convolution(error);`
6 `norm_error = error - avg_error;`
7 P_{i+1} `=` P_i `-` `norm_error` $\cdot A$`;`

The process is illustrated in 2D in figure 3.

The function `normal_between(`(x_s, y_s)`,`(x_t, y_t)`)` returns the normal from the normal map N_{comb} between (x_s, y_s) and (x_t, y_t) if they are diagonal neighbors, and the normalized average of the two normals in between, if they are not (see Fig. 2).

The variable denoted ϵ in the code tells by how much point $P_i[x_t, y_t]$ has to be shifted along $A[x_t, y_t]$ in order for the straight line between $P_i[x_t, y_t]$ and its neighbor $P_i[x_s, y_s]$ to be perpendicular to n. The sum of the `weight` terms of all neighbors has to be one or less. The `weight` of diagonal neighbors has been chosen as half as much as the weight of direct neighbors in our case.

The error is normalized prior to the computation of P_{i+1}, as we are only interested in its

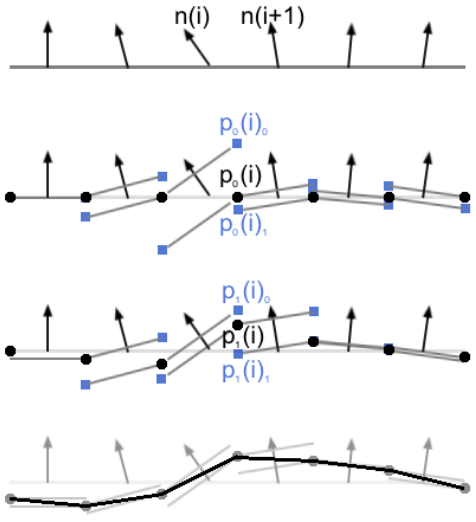

Figure 3: An illustration of our surface reconstruction algorithm as applied to a 2D normal map. The black circular dots represent the current positions, while the blue square dots are where the neighboring texels at their current positions require the positions to be. Please note that all 2D normal maps in fact correspond to valid 2D-surfaces (ie. piecewise linear functions), which is not the case with all 3D normal maps.

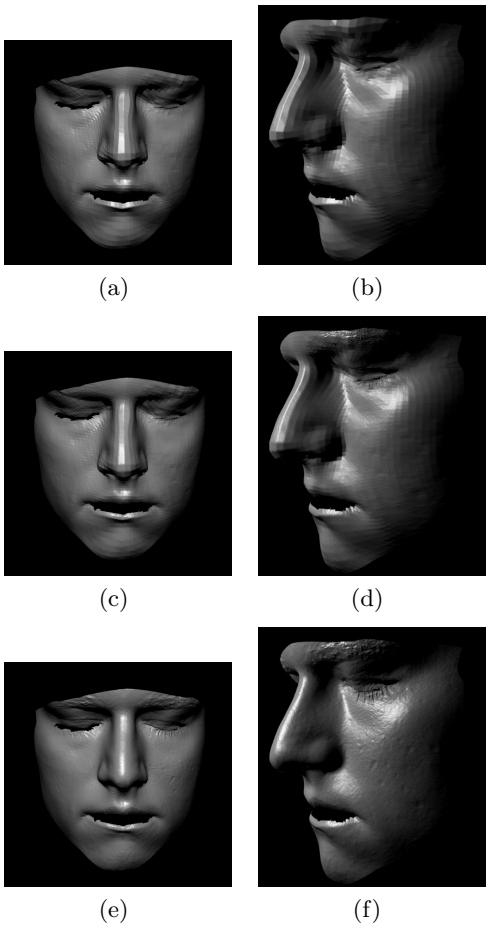

Figure 4: The surface reconstruction process using a 512×512 normal map and a 128×128 mesh, resulting in a 512×512 mesh. The initial surface (a, b), the surface after one iteration (c, d) and after 41 iterations (e, f).

high frequency component - on a coarser scale, the mesh is assumed to be correct.

Depending on texture resolution, between 20 and 50 such iterations are required to approach a state of equilibrium.

6 RESULTS

Our method allows for the reconstruction of high resolution surface detail of human faces using only very limited information as input. For this reason, the method is also susceptible to missing data, in the form of shadows cast by the face onto itself. This is problematic, because both the positions of the light sources and the shape of the face casting the shadows are only known up to a certain degree of accuracy.

The four flash lights were mounted approximately 35 degrees left and right and 15 degrees up and down in front of the person to scan. That arrangement has been chosen to minimize areas shadowed under more than one light. Although points illuminated by only two or less of the four lights can be filled in using the original vertex normals as a fallback, care has to be taken to calculate the shadows using an adequate margin of error. If shadowed texels are not filtered out strictly enough, they will influence the resulting normals. At the same time, we can not afford to lose too many lit texels in the proximity of shadowed regions. The artifacts arising from inadequately suppressed shadows are illustrated in Fig 6.

The estimated normals for all three color channels are shown in Fig 7. Note that the normals based on the red channel are much smoother than those based on the blue channel. This can be explained by the more extensive scattering of red light in the deeper layers of the skin (see [Jensen et al., 2001]).

Comparisons between renderings created using geometric normals and our estimated normal maps can be seen in Fig. 5 and 8. The geometric normals have been computed at each vertex by averaging the normals of nearby triangles. The algorithm takes about eleven minutes on an Intel Core2 6600 2.40GHz for one 1024×512 normal map. Overall, the method provides visually convincing results, while the cost of the required additional hardware remains relatively low (below 1000 USD, given an existing structured light scanner).

6.1 Acknowledgment

This work was partially funded by the NCCR COME project number 5005-66380.

REFERENCES

[Barsky and Petrou, 2001] Barsky, S. and Petrou, M. (2001). Colour photometric stereo: simultaneous reconstruction of local gradient and colour of rough textured surfaces. *Eighth IEEE International Conference on Computer Vision*, 2:600–605.

[Borshukov and Lewis, 2003] Borshukov, G. and Lewis, J. (2003). Realistic human face rendering for" The Matrix Reloaded". *International Conference on Computer Graphics and Interactive Techniques*, pages 1–1.

[Haro et al., 2001] Haro, A., Guenter, B., and Essa, I. (2001). Real-time, Photo-realistic, Physically Based Rendering of Fine Scale Human Skin Structure. *Rendering Techniques 2001: Proceedings of the Eurographics Workshop in London, United Kingdom, June 25-27, 2001*.

[Jensen et al., 2001] Jensen, H., Marschner, S., Levoy, M., and Hanrahan, P. (2001). A practical model for subsurface light transport. *Proceedings of the 28th annual conference on Computer graphics and interactive techniques*, pages 511–518.

[Ma et al., 2007] Ma, W., Hawkins, T., Peers, P., Chabert, C., Weiss, M., and Debevec, P. (2007). Rapid acquisition of specular and diffuse normal maps from polarized spherical gradient illumination. *Submitted to EGSR*.

[Nehab et al., 2005] Nehab, D., Rusinkiewicz, S., Davis, J., and Ramamoorthi, R. (2005). Efficiently combining positions and normals for precise 3D geometry. *Proceedings of ACM SIGGRAPH 2005*, 24(3):536–543.

[Weyrich et al., 2006] Weyrich, T., Matusik, W., Pfister, H., Bickel, B., Donner, C., Tu, C., McAndless, J., Lee, J., Ngan, A., Jensen, H., et al. (2006). Analysis of human faces using a measurement-based skin reflectance model. *International Conference on Computer Graphics and Interactive Techniques*, pages 1013–1024.

APPENDIX

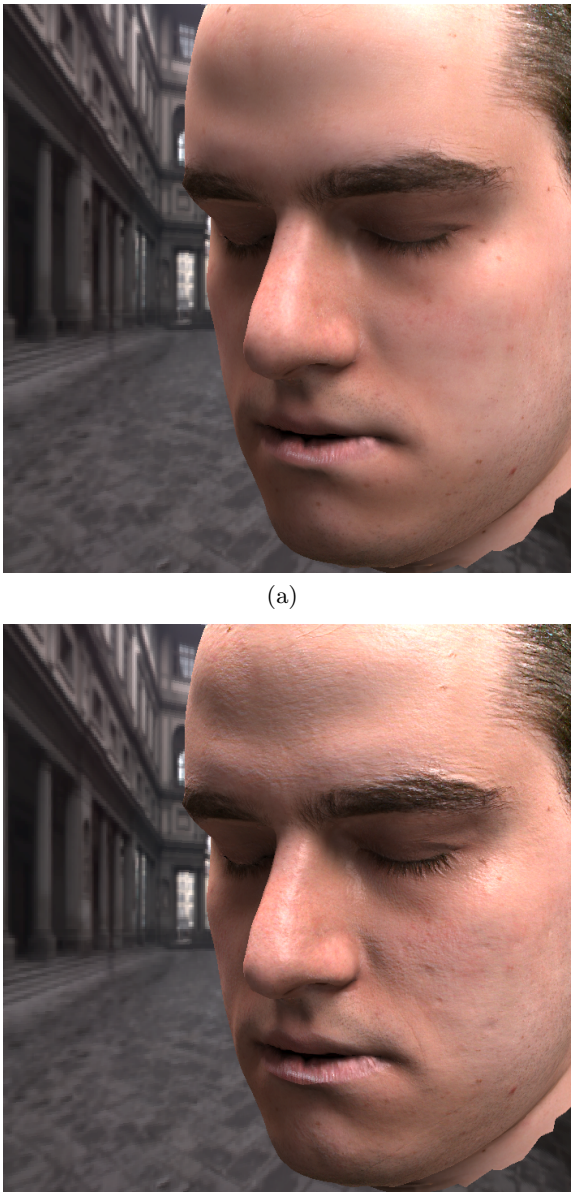

(a)

(b)

Figure 5: Renderings of a face under omnidirectional lighting from the Uffizi light probe. The original geometric normals can be seen in (a) and the highly detailed normals obtained through our method in (b).

(a) (b)

Figure 6: Possible failure scenarios: points inside shadows are not discarded strictly enough (a), so the shadow of the nose leaves an imprint on the normal map, or they are discarded too strictly (b), creating a gap in the normal map at the center of the nose.

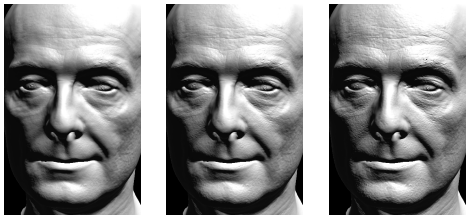

(a) (b) (c)

Figure 7: Shaded normal maps for the red (a), green (b) and blue (c) channel. Note that the perceived smoothness of the surface increases with greater wavelength.

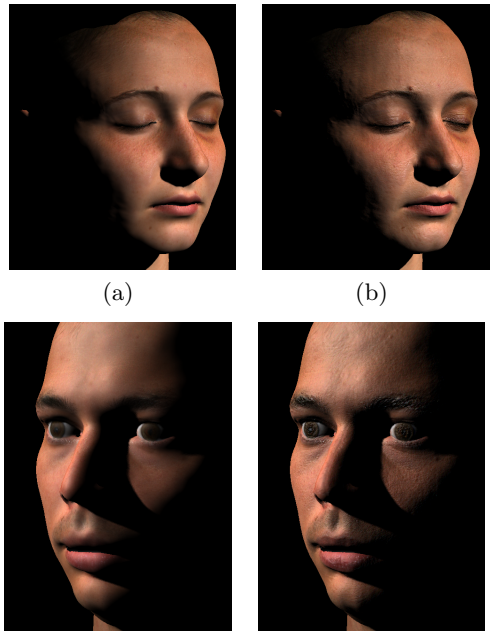

(a) (b)

(c) (d)

Figure 8: More renderings under a point light using geometric normals (a, c) and our normal map (b, d).

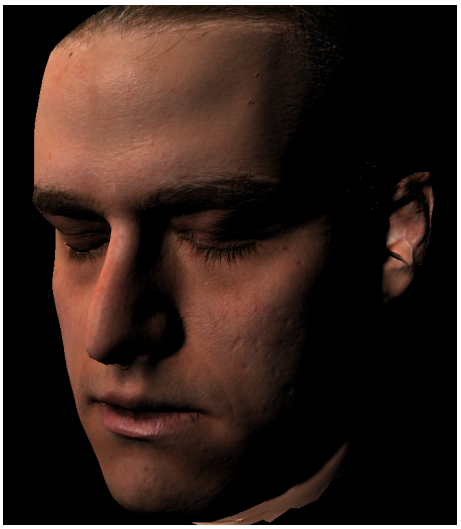

(a)

(b)

(c)

Figure 9: Renderings of normal mapped heads under a point light.